Journal of Magnetic Resonance 304 (2019) 53–61

Contents lists available at ScienceDirect

Journal of Magnetic Resonance

journal homepage: www.elsevier.com/locate/jmr

Effect of linewidth on estimation of metabolic concentration when using water lineshape spectral model fitting for single voxel proton spectroscopy at 7 T

Donghyun Hong [a,*], Jack J.A. van Asten [b], Seyedmorteza Rohani Rankouhi [a], Jan-Willem Thielen [a,c], David G. Norris [a,d]

[a] Erwin L. Hahn Institute for Magnetic Resonance Imaging, University of Duisburg-Essen, Essen, Germany
[b] Department of Radiology and Nuclear Medicine, Radboud University Medical Center, Nijmegen, Netherlands
[c] Department for Psychiatry and Psychotherapy, Faculty of Medicine, University of Duisburg-Essen, Essen, Germany
[d] Donders Institute for Brain, Cognition, and Behavior, Radboud University, Nijmegen, Netherlands

ARTICLE INFO

Article history:
Received 23 September 2018
Revised 14 April 2019
Accepted 8 May 2019
Available online 9 May 2019

Keywords:
B_0 field inhomogeneity
Fitting freedom
Single-voxel spectroscopy
Ultrahigh field
Water lineshape fitting model

ABSTRACT

Good B_0 field homogeneity is considered an essential requirement to obtain high-quality MRS data. Many commonly used spectral fitting methods assume that all metabolite signals have Lorentzian or Gaussian shapes. However, B_0 inhomogeneity can both broaden the linewidth and modify the lineshape. In this study, it is hypothesized that a realistic metabolite fitting model, which accounts for B_0 homogeneity on the basis of the water lineshape, will improve the accuracy of estimation of metabolite concentrations. *In-vivo* water suppressed/unsuppressed single voxel spectroscopy signals were acquired under three different B_0 field homogeneity regimes. Individual realistic basis sets were created for each acquisition. Frequency-domain spectral fitting with LCModel was used to quantify the metabolite concentrations with fitting uncertainties given in terms of the Cramer-Rao lower bound. The quantification results obtained using the water lineshape basis set yielded similar concentrations independent of linewidth and showed a larger fitting error as the linewidth increased. The conventional approach, however quantifies metabolite concentrations with greater variations despite showing a supposedly improved fitting quality. The water lineshape basis set achieved single voxel spectroscopy accuracy that is less sensitive to the linewidth compared to the conventional spectral fitting method for the range of linewidths used in this study, but the precision deteriorated with worsening B_0 field inhomogeneity. The beneficial effect was ascribed to a reduction in the number of degrees of freedom when using the water lineshape to generate the basis set.

1. Introduction

Nuclear magnetic resonance (NMR) spectroscopy is a widely used non-invasive technique to obtain biochemical information from the human brain. A fundamental objective of NMR spectroscopy is to measure metabolite levels within the voxel of interest (VOI). To this end, spectral fitting is commonly used along with various quantification algorithms [1–3]. Spectral fitting is challenging because metabolite signals have low concentrations and overlapping resonances. Moreover, unwanted factors, such as B_0 field inhomogeneity and eddy currents, distort experimental lineshapes while simultaneously reducing the signal-to-noise ratio (SNR) [4]. Above all, a favorable B_0 field homogeneity is an essential requirement because it directly affects the spectral lineshape. An inhomogeneous B_0 field leads to SNR reduction. It can both broaden the linewidth and cause it to deviate from a Lorentzian form. Although B_0 field shimming is a pre-requisite for spectral acquisition, shimming is not invariably successful and the well-shimmed B_0 field can be destroyed during the spectral acquisition. In particular, B_0 inhomogeneity at the ultrahigh field (UHF, 7 T and above) is more severe owing to magnetic susceptibility effects. While spectroscopy at UHF shows improved performance in detecting metabolites with enhanced SNR and spectral resolution due to the high spectral dispersion and increased sensitivity [5], robust shimming techniques, such as higher order [6] and dynamic shimming [7] methods have been proposed to address the poorer B_0 inhomogeneity.

* Corresponding author at: Erwin L. Hahn Institute for Magnetic Resonance Imaging, University of Duisburg-Essen, Kokereiallee 7, Building C84, UNESCO World Heritage, Zeche Zollverein, 45141 Essen, Germany.

E-mail address: donghyun.hong@uni-due.de (D. Hong).

https://doi.org/10.1016/j.jmr.2019.05.002
1090-7807/

Most quantification methods assume that the ideal spectral lineshape can be represented using a Lorentzian function, which corresponds to exponential decay in the time domain. When experimental spectra have this ideal form with a narrow linewidth, the best quantification performance can be expected. Otherwise, additional steps are required to correct the lineshapes. Hitherto, there have been many attempts to convert arbitrary lineshapes into an analytic lineshape. We can broadly classify the previously proposed methods for correcting distorted lineshapes into those that use a reference lineshape and those that do not.

In the first approach, imperfect lineshapes due to B_0 field inhomogeneity or eddy currents are corrected by de-convolving the reference lineshape in the time domain. Some representative methods include QUALITY deconvolution [8] and SPREAD [9,10], which use field mapping for B_0 field inhomogeneity, eddy current correction (ECC) [11] for the distortion due to eddy currents, and QUECC, which is a combination of QUALITY deconvolution and ECC [12] with advantages of both.

As mentioned earlier, in the second classification, a reference lineshape is not required. Convolution with an additional parametric or non-parametric lineshape is used. For instance, a lineshape obtained by the combination of Lorentzian and Gaussian lineshape functions, namely the Voigt lineshape, compensates the arbitrary lineshape [13], or model-free fitting methods [14,15] can be used to quantify metabolites using non-analytical lineshapes. The self-deconvolution method can in principle correct the distorted lineshape into an analytic form [16,17]. However, in these approaches, many degrees of freedom need to be regularized by additional strategies such as the regularized lineshape deconvolution [18,19], or the regularized semi-parametric model [20]

As multiple factors can cause the experimental lineshape to deviate from a Lorentzian form, it is challenging to precisely correct the distorted lineshapes using regular mathematical algorithms. In addition, while correcting a resultant spectrum, there is a risk of losing critical spectral information and compromising the SNR. In this study, we hypothesize that a realistic metabolite fitting model considering the B_0 homogeneity can be used to better estimate the metabolite concentration, thus obtaining fitting results that are less dependent on high B_0 field homogeneity. Similar approaches that utilize water reference lines in order to compensate for B_0 field inhomogeneity have previously been reported [15,21,22], the combination with LCModel, which is one of the most widely used quantification approaches, combined with human brain spectroscopy at 7 T remains unexplored.

The aim of this study is to examine the degree to which the LCModel analysis is dependent on the linewidth, thus potentially improving spectral measurement in the presence of relatively broad spectral lines.

2. Materials and methods

2.1. Basic concept of model fitting

The commonly used spectral fitting methods, which work in the frequency domain, such as, LCModel [14], MIDAS [23], TARQUIN [2], TDFDFit [15], and ProFit [24], quantify the relative metabolic concentrations with similar algorithms that utilize time domain fitting models in order to exploit advantages of the time domain with regard to the frequency shift, eddy current, phase and lineshape [25]. Assuming that the experimental signal is a linear combination of the metabolite signals, the metabolite levels are determined by combining each of the simulated signals. In the case of LCModel, which is used in this study, model spectra are fitted to each metabolic signal using the Levenberg–Marquardt non-linear fitting algorithm [26], which involves solving an optimization problem. The non-parametric baseline, lipid, and macromolecule (MM) signals are additionally fitted using the cubic *b*-spline simultaneously.

The ideal spectral profile of each metabolite under given experimental conditions can be predicted using quantum-mechanical calculations [27], and these are widely accepted as prior knowledge for spectral fitting. This is the basis of spectral fitting using simulated metabolite spectra, which has proven to be a powerful approach to quantify metabolite levels. However, thus far, potential spectral lineshape modifications due to B_0 field inhomogeneity have been widely ignored in the spectral models, even though they may lead to inaccurate quantification. Instead, researchers widely depended on additional correction steps before fitting [8,28,29], or an additional non-parametric function during spectral fitting procedures [3,15,30–32].

The water lineshape fitting method proposed in this study can be used to directly fit the *in-vivo* spectra with their corresponding realistic lineshape models. Several assumptions are made in this approach: (1) that the lineshapes of all the metabolites are identical, and are defined by the envelope of the free induction decay (FID), and are equal to that of the water signal. (2) The chemical shifts and J-coupling for each metabolite can be specified. From these assumptions, we designed realistic metabolite models that meet these conditions using the water lineshape. We then used a water lineshape basis set for spectral fitting without modifying the resultant *in-vivo* spectra.

2.2. Data acquisition

MRI and MRS were performed on ten healthy human subjects (eight males; two females; 31.70 ± 4.99 years old) using a 7 T whole-body scanner (Magnetom, Siemens, Erlangen, Germany) with a 1 Tx/32 Rx head coil (Nova Medical, Wilmington, MA). Written consent was collected from each subject. The experimental protocol was approved by our institutional review board (IRB).

T_1 weighted images with 3D magnetization-prepared radiofrequency pulses and rapid gradient-echo (MPRAGE) [33] were acquired before the spectroscopic scan as an anatomical reference. Spectroscopy was performed at the occipital cortex using the semi-localization by adiabatic selective refocusing (semi-LASER) sequence [34,35] with the following parameters: 8 ml isotropic voxel volume; echo time (TE) = 38 ms; repetition time (TR) = 4500 ms; number of averages = 64; bandwidth (BW) = 3500 Hz; and spectral resolution = 1024 data points.

The MRS acquisitions were repeated under three different B_0 field homogeneity conditions. The target ranges of the water linewidth under the three conditions were poor (30–40 Hz), medium (20–30 Hz), and good (10–20 Hz). The B_0 field homogeneity was modified by repeating FASTESTMAP [36] until the water linewidth reached the target condition starting at the poor linewidth and then iterating the shimming procedure so that all three bins were measured. In the situation where the initial linewidth was narrower than the target range after the first attempt by FASTESTMAP, we manually adjusted the shimming by changing the first order linear gradients (A11, B11, and A10) and second order shim currents (A20, A21, B21, A22, and B22) by the same percentage to increase the linewidth. We acquired the corresponding water lineshape by turning off the water suppression in each shim case. For the water signal acquisition, the transmitter (TX) frequency was switched to water. The number of averages for water signal acquisition was 16. The remainder of the acquisition parameters (e.g., acquisition sequence, TE, TR, B_0 field homogeneity, and spectral resolution) were kept constant between shim conditions.

2.3. Data processing

The model spectra of 22 metabolites: alanine (Ala), aspartate (Asp), glycerophosphocholine (GPC), choline (Cho), phosphocholine (PCh), creatine (Cr), phosphocreatine (PCr), gamma-aminobutyric acid (GABA), glucose (Glc), glutamine (Gln), glutamate (Glu), glycine (Gly), glutathione (GSH), myo-inositol (mI), lactate (Lac), N-acetyl aspartic acid (NAA), N-acetyl aspartyl glutamate (NAAG), phosphoethanolamine (PE), serine (Ser), scyllo-inositol (Scyllo), and taurine (Tau), which are typically detectable in the human brain using proton spectroscopy, were created according to previously reported chemical shifts and coupling constants [37,38]. The NMRSIM module of the TOPSPIN suite (Ver. 3.6, Bruker, Rheinstetten, Germany) was used to simulate each metabolite with identical acquisition sequence and parameters that include identical RF timing and pulse profiles that were used for the *in-vivo* acquisition.

A conventional basis set was simply created by combining the simulated metabolite models. This conventional basis set was used for all *in-vivo* results. The water lineshape basis set was created individually for each acquisition by multiplying the corresponding water signal with the signal profile of each metabolite in the time domain. The water signal was normalized to its maximum intensity to exclude the effect of reference voltage variations. As the amplitude of the water signal was the same for all cases, this water lineshape basis set shows identical signal amplitude ratios in every case. The only difference was in terms of the lineshape. To create the water lineshape basis set, an additional water signal is required at the expense of prolonged scan time. However. the water signal is widely required as a routine protocol to have an absolute concentration quantification and an ECC.

2.4. Data analysis

To verify the spectral quality under the three different B_0 field homogeneity conditions, we measured the linewidth at the half maximum points from the water signal. The SNR of the *in-vivo* spectrum was also measured from the NAA peak and the white noise area at from 7 to 9 ppm for each case.

Linewidths of metabolites and water were also compared in order to determine whether differences in T_2 had a discernible effect on the line width. Full-width at half maximum (FWHM) of the water un-suppressed signal and clearly visible metabolite signals at 3.2 ppm (tCho: Cho + PCh + GPC), 3 ppm (tCr: Cr + PCr) and 2 ppm (tNAA: NAA + NAAG) for the three different shim conditions were measured with jMRUI software (ver. 6.0, http://www.jmrui.eu) [1].

LCModel (Version 6.3-1L, SW Provencher, Oakville, Canada) was used to quantify the absolute metabolic concentration and estimate quantification uncertainties, using the Cramer–Rao lower bound (CRLB), which is defined as the lowest possible standard deviation of all unbiased model parameter estimates obtained from the *in-vivo* data [39,40]. For LCModel, the mean-squared error of any unbiased estimator, which denotes spectral parameters such as metabolite concentrations, linewidth, and phase, is lower bounded by the square roots of the diagonal entries of the inverse of the Fisher information matrix, which essentially describes the correlations between spectral parameters [41]. As an index for the reliability of detection, decreased CRLB value is interpreted as denoting increased reliability for metabolite detection [3]. Prior to the spectral fitting, frequency referencing, 0^{th} and 1^{st} order phasing and ECC were performed by LCModel. Individually acquired spectra over coil elements and averages were aligned and combined by the 1^{st} point signal weighting method [42]. Spectral fitting was performed with two different basis sets, namely the conventional basis set and the water lineshape basis set with water scaling using individual water signals, which were acquired additionally in all cases. The LCModel parameter that controls the flexibility of the spline baseline (DKNTMN) was set to 0.1 as a default value. In order to explore the effect of the baseline spine function, the conventional basis set approach was also analyzed with DKNTMN set to values that gave a similar level of baseline fluctuation as that of the water lineshape basis set. For the lineshape, we did not modify the fitting parameter that controls linewidth (i.e. DEEXT2 and DESDT2). In addition, MM and lipid models were not considered in the baseline. However, since the lineshape and linewidth of the MM and lipid are not mathematically predictable, we used internally provided non-parametric spectral models for fitting MM and lipid signals. Therefore, we did not apply the water lineshape to the spectral models for MM and lipid. As LCModel recommends [43], we also assumed that water concentrations of gray matter (GM), white matter (WM), and cerebrospinal fluid (CSF) are 43,300, 35,880, and 55,556 mM, respectively. Quantified metabolic concentrations were expressed as mmol per kg wet weight. To exclude individual variations, metabolite concentrations were individually corrected by averaged concentrations over 10 subjects as estimated at the good shim condition. For this step, we assumed that the estimated metabolite concentrations from good shim data were close to the actual concentration. Metabolite concentrations and CRLB were compared between the conventional and water lineshape methods.

The typical acceptance value for the CRLB was under 30%, as recommended by other spectroscopy studies [44]. Nevertheless, we only excluded CRLB values of 999%, which indicate the situation where metabolite was not detected. Previously, Kreis has warned that arbitrarily thresholded data may cause bias [45]. Therefore, we used a cut off as 998% as a previous study used [46] in order to include as many metabolites as possible and show CRLB changes between the conventional and water lineshape methods. An additional comparison was performed for the number of metabolites that was detected with CRLB below 30% and between 31 and 998% by the two approaches. The statistical significance was determined by performing ANOVA analysis between three different linewidth groups, and two methods using SPSS (Ver. 22, IBM, NY). The null hypothesis was that there is no difference between the results obtained under different B_0 homogeneity conditions.

3. Results

The water linewidths were 12.65 ± 2.23, 22.65 ± 2.32, and 36.16 ± 3.06(Hz) corresponding to the good, medium, and poor field homogeneity conditions, respectively. The overall range of water linewidth was from 9.98 to 39.52 Hz. The SNRs of the *in-vivo* spectra were 309.89 ± 77.30, 235.68 ± 59.44, and 184.61 ± 28.20 corresponding to the good, medium, and poor field homogeneity conditions, respectively (see Fig. 1).

Table 1 summarizes measured linewidths for the water and metabolite signals. For all shim conditions, we found comparable linewidths between the water and selected metabolite signals

Fig. 2 shows the steps for the spectral fitting model creation. The water lineshapes that acquired under each field homogeneity condition from one representative subject are compared, as shown in Fig. 2A. As the B_0 field in the voxel becomes heterogeneous, the water lineshape changes from a Lorentzian form and may become asymmetrical as shown for the broadest line. Fig. 2B shows the NAA profile, which is calculated on the basis of spectral simulation using identical acquisition parameters to those used *in-vivo*. Fig. 2C shows a comparison of the modified basis sets under each field condition. The basis set was created by multiplying its corresponding water lineshape (see Fig. 2A) with a simulated metabolite profile (see Fig. 2B). The linewidth of the combined spectrum was

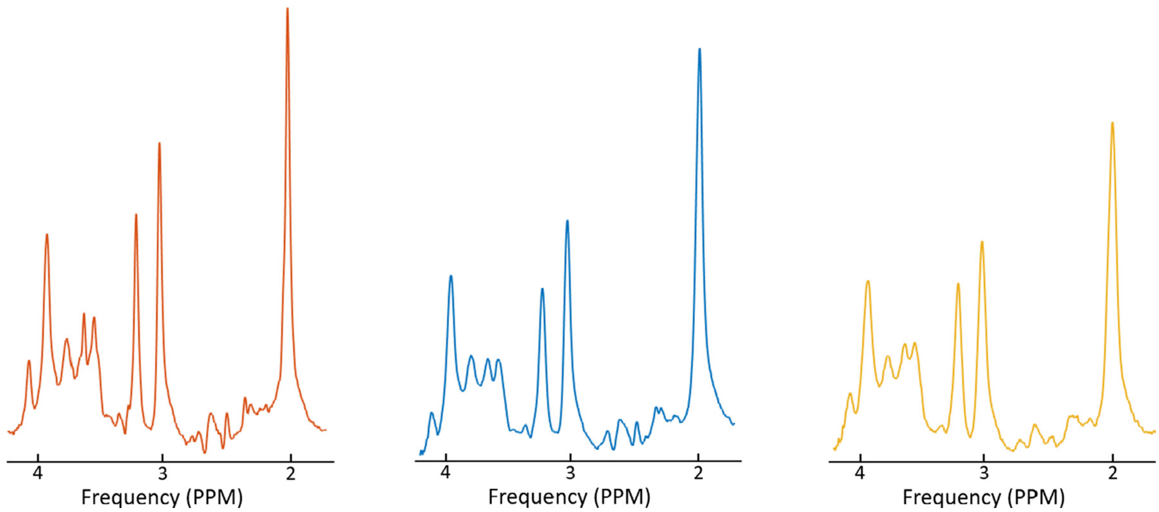

Fig. 1. Comparison of *in-vivo* spectra under three B_0 field conditions from one representative subject. The mean linewidths measured from the water signal in the real mode were 12.65 ± 2.23, 22.65 ± 2.32, and 36.16 ± 3.06 (Hz) corresponding to the good (red), medium (blue), and poor (yellow) field homogeneity conditions, respectively. Their corresponding mean SNRs were 309.89 ± 77.30, 235.68 ± 59.44, and 184.61 ± 28.20, respectively. (For interpretation of the references to color in this figure legend, the reader is referred to the web version of this article.)

Table 1
Linewidth comparison for water and clearly visible metabolites: tCho, tCr, and tNAA under three different shim condition, given as mean ± SD in Hz. Linewidths of the metabolites showed a good agreement with that of the water peak.

	Good	Medium	Poor
Water	12.7 ± 2.2	22.7 ± 2.3	36.2 ± 3.1
tCho	13.7 ± 2.5	24.4 ± 2.5	37.7 ± 1.4
tCr	13.5 ± 2.1	26.0 ± 2.6	39.3 ± 1.7
tNAA	12.1 ± 1.1	24.4 ± 2.9	37.5 ± 0.7

dominated by that of the water. Therefore, the relatively narrow linewidth of the simulated spectrum did not affect the linewidth of the combined signal.

Fig. 3 compares the average absolute concentration (A) and CRLB (B) as estimated using the conventional basis set, the conventional basis set with restricted baseline estimation and the water lineshape basis sets, for all metabolites quantified by LCModel fitting. When DKNTMN, which controls the baseline flatness, was set in the range from 0.20 to 0.29, the baseline of the conventional basis set showed similar fluctuation levels to those of the water lineshape basis set. Metabolites that were only detected by one method were excluded. In comparison with the conventional basis set, the water lineshape basis set tends to quantify the metabolite concentrations with lower variance for all three shimming groups. However, the water lineshape basis estimated metabolites with a greater fitting error for most metabolites. When the restricted baseline estimation is used, the conventional basis set approach estimates metabolite concentrations with a smaller variation and fitting error in comparison with the soft baseline approach for most metabolites.

Fig. 4 shows the comparison of the summed metabolite concentrations (A) and average CRLB (B) overall metabolites for the three different approaches under the three different static field conditions. In this comparison, we included all detected metabolite in order to compare overall changes of concentrations and CRLBs by two methods. Below a linewidth of 30 Hz, the two methods did not show a statistical difference for either index according to the *p-value*, which was greater than 0.05. In the poor shim group, the three approaches showed statistically significant differences for both the concentration and the CRLB. Even if summed metabolite concentrations are not significantly different between three

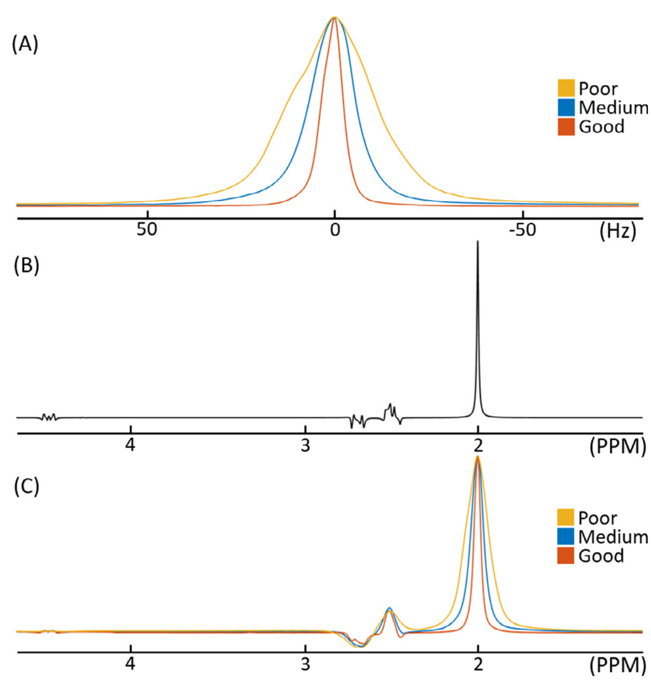

Fig. 2. (A) Comparison of water lineshapes under three different B_0 field homogeneity conditions, namely good (red: linewidth of 11 Hz), medium (blue: 24 Hz), and poor (yellow: 39 Hz), from one representative subject. (B) Simulated NAA profile, which is widely used as a spectral fitting model. (C) Comparison of modified basis sets of NAA for the water lineshape fitting approach under each field condition. The water lineshape basis set is created by multiplying its corresponding (A) water signal with a (B) simulated metabolite profile in the time domain. (For interpretation of the references to color in this figure legend, the reader is referred to the web version of this article.)

approaches below a linewidth of 30 Hz (*p-value* > 0.05), the water lineshape approach showed a significantly lower variation than those of the conventional method and the conventional approach with a restricted baseline estimation for the concentration estimation. This effect was observable for all shimming groups. In addition, when the restricted baseline estimation was used, the conventional basis set method showed a smaller variation for both concentration and CRLB estimations compared to the smooth

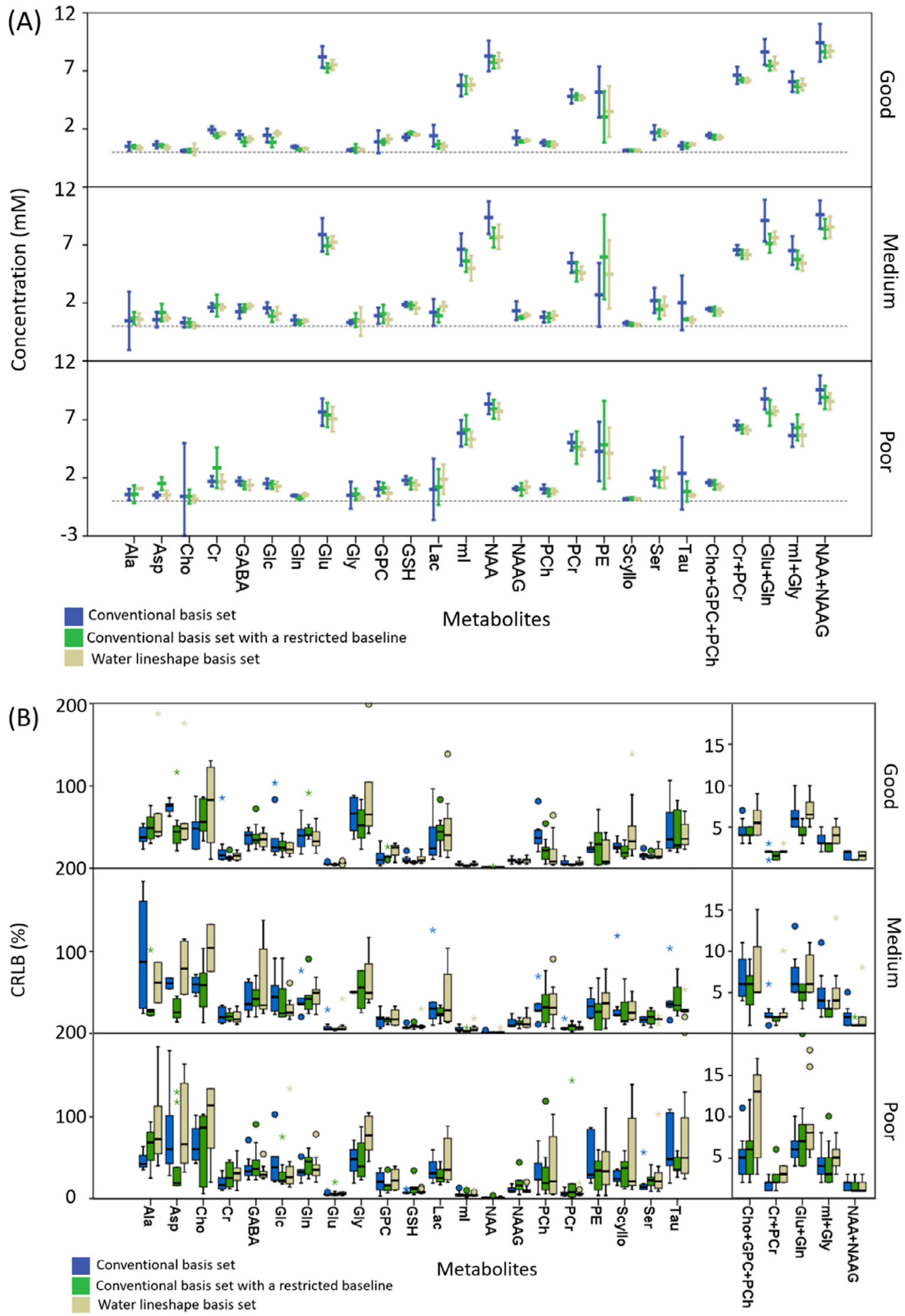

Fig. 3. Estimated average absolute concentration with 95% confidence intervals (shown as error bars) (A) and CRLB (B) under three different shimming conditions for the conventional basis set, conventional basis set with a restricted baseline, and the water lineshape basis set, for all metabolites quantified by LCModel fitting. In comparison with the conventional basis set, the water lineshape basis set tends to show lower concentration and higher CRLB values for most metabolites. The dotted line of Fig. 3A indicates zero mM. Note that metabolites detected by all three approaches were only compared.

baseline estimation. However, these improvements were inferior to those of the water lineshape basis set in terms of stability. This effect was observable for all shimming groups.

A one-way analysis of variance (ANOVA) showed that average metabolite concentrations estimated using the conventional basis set were significantly different between shim groups ($F(2,30) = 5.184$, $p = 0.014$). On the other hand, the water lineshape basis set estimated metabolites concentrations similarly over groups ($F(2,30) = 1.484$, $p = 0.248$). The averaged CRLBs over all metabolites that were estimated with the conventional basis set and the water lineshape model basis set increased as the static field became more heterogeneous (see Fig. 3B).

However, the average CRLB obtained using the water lineshape basis set increased more steeply than those of the conventional basis set. ANOVA results showed that the estimated CRLBs by the conventional basis set are not significantly different between shim groups ($F(2,30) = 1.807$, $p = 0.187$); whereas, those by the water basis set are significantly different ($F(2,30) = 5.974$, $p = 0.008$).

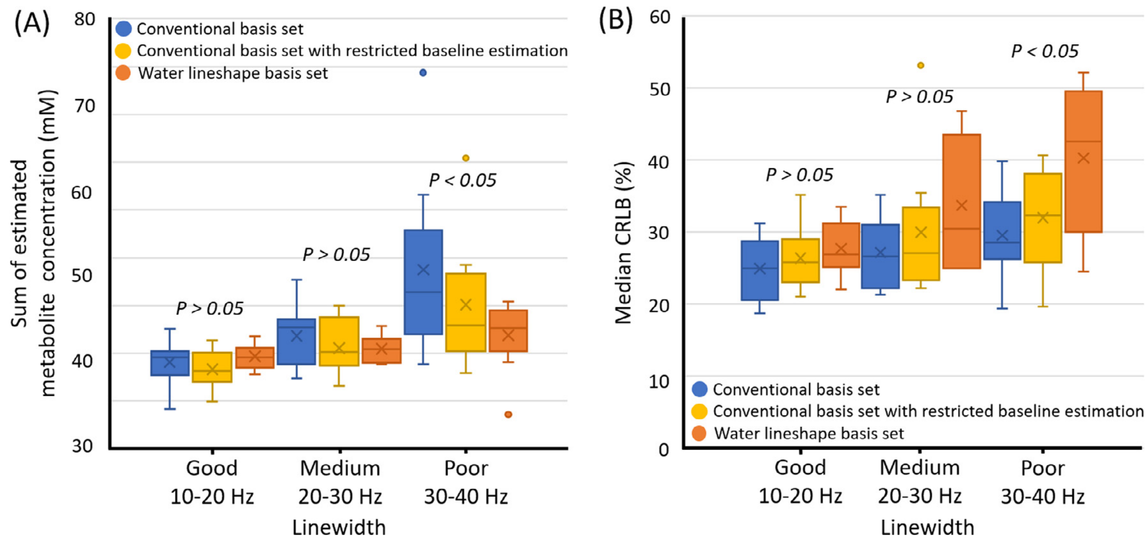

Fig. 4. Comparisons of summed metabolite concentration (A) and median CRLB (B) over estimated metabolites by three approaches between groups: good (10–20 Hz), medium (20–30 Hz), and poor (30–40 Hz) from the results shown in Fig. 3. For linewidths of 10–30 Hz, the two methods did not show a statistical difference for both indexes, with *p-values* greater than 0.05. However, for 30–40 Hz linewidth, the three approaches showed statistically significant differences for both the concentration and CRLB.

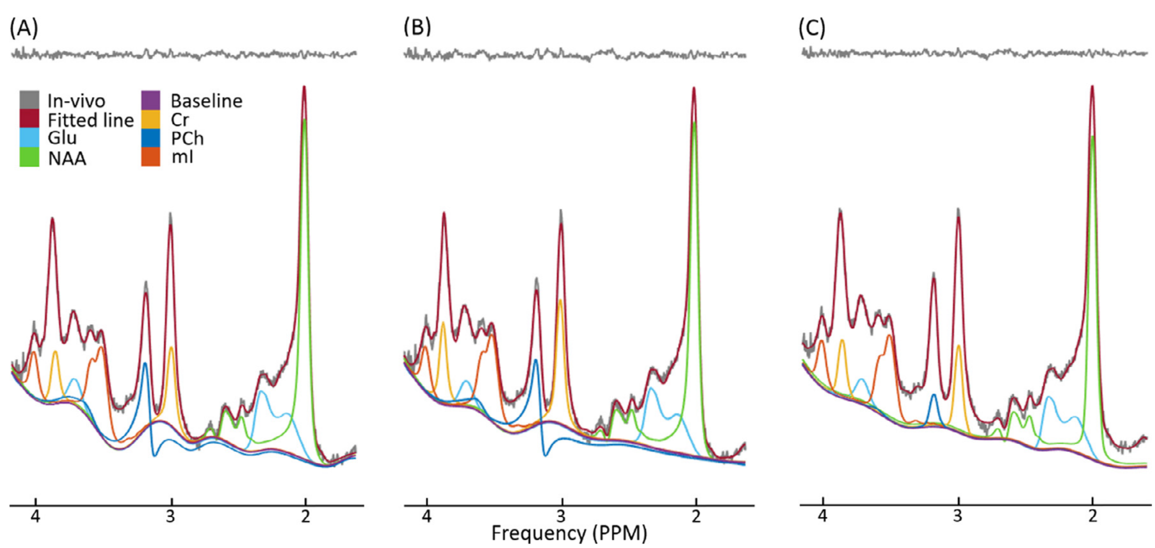

Fig. 5. LCModel results for an exemplary spectrum, acquired with a linewidth of 39 Hz, fitted by (A) the conventional basis set, (B) the conventional basis set with restricted baseline estimation and (C) the water lineshape basis set. Fitted lines, baselines, residuals and the highest concentration metabolites (Glu, NAA, Cr, PCh, and mI) are shown. The different baselines correspond to loose (A) and tighter (B and C) baseline constraints which mean that more degrees of freedom are required to fit (A). The fluctuating baseline generated from the conventional basis set made it possible to more closely fit the *in-vivo* lines than was possible for the water lineshape basis set. However, in this example, the oscillating baseline causes unrealistic signal phasing (for example see PCh line (blue) in Fig. 5A). In general, the estimates of metabolite concentration are higher for the conventional basis set. The restricted baseline from the conventional basis set with constrained regularization still showed the phasing problem even if its level is decreased and there remained a higher level of the residual signal in comparison with the other two approaches. (For interpretation of the references to color in this figure legend, the reader is referred to the web version of this article.)

Fig. 5 shows the LCModel fitting results for an exemplary spectrum, with a linewidth of 39 Hz fitted using the conventional basis set, the conventional basis set with a restricted baseline estimation and the corresponding water lineshape basis set. This shows the fit for the most highly concentrated metabolites (NAA, PCh, Cr, Glu, and mI) and the baseline, for both quantification approaches. The conventional basis set showed a loose baseline constraint (Fig. 5A) and when restricted baseline estimation was used, the conventional basis set showed a similar baseline fluctuation level to that of the water lineshape basis set (Fig. 5B). Water lineshape basis set showed a tighter baseline (Fig. 5C) in comparison with that of the conventional basis set. Different flexibility of the baseline constraint indicates that more degrees of freedom are required to fit with the conventional basis set. The fluctuating baseline generated from the conventional basis set made it possible to more closely fit the *in-vivo* lines than was possible for the water lineshape basis set. However, in this example, the oscillating baseline causes unrealistic signal phasing (for example see PCh line (blue) in Fig. 5A). In general, the estimates of metabolite concentration are higher for the conventional basis set.

The average number of detected metabolites averaged over subjects for the two different basis sets are compared between three shimming groups in Fig. 6. As shimming conditions get worse, both the number of detected metabolites decreased. The total number of metabolites detected was higher for the water lineshape approach for all shim groups, but the number with CRLB < 30% was the same

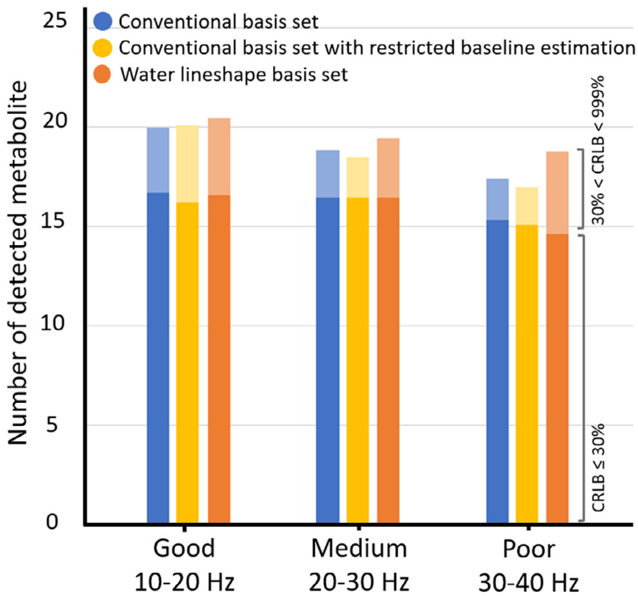

Fig. 6. Comparison of the average number of detected metabolites for the conventional basis set and the water lineshape basis set under three shimming conditions. For all shimming conditions, the water lineshape basis set detected more metabolites than the conventional basis set. However, the number of detected metabolites by the water lineshape basis set with CRLB < 30% was the same or less than that detected by the conventional basis set for all groups. When a restricted baseline estimation was used, the conventional basis set detected decreased number of metabolites.

or less. When a restricted baseline estimation was used, the conventional basis set detected a decreased number of metabolites than with the other two approaches for linewidths of 20–30 Hz.

4. Discussion

This study demonstrated the effect of linewidth on estimates of metabolite concentration when using the realistic spectral model fitting. Lineshape modifications using the reference lineshapes from the water signal [15,22] or the B_0 map [21] for the spectral fitting model have previously been reported. Similar to these previous studies, modified spectral models using the water lineshape in this study also improved the accuracy and stability of spectral quantification for the B_0 field inhomogeneity induced broad linewidth. For most metabolites, the water lineshape fitting method estimated more consistent metabolite concentration levels with smaller variations compared to the conventional fitting method, for the different field homogeneity conditions tested. However, the conventional fitting method had numerically lower values of the CRLB parameter.

A common limitation of spectral fitting methods is their lack of uniqueness [47]. The objective of non-linear or linear least square fitting is to minimize the squared deviations from the mean (SDM) between the spectral models and the experimental spectrum without considering practical metabolite levels. Therefore, spectral fitting is always at risk of over- (detecting wrong signals) and under- (missing correct signals) fitting, in the situation that *in-vivo* spectra do not have enough information for accurate quantification due to the inhomogeneous B_0 field. This problem was also observed in our spectral fitting results. If we assume that the spectral quantification result of the narrow linewidth spectrum, which was acquired under homogenous B_0 field conditions, is closest to the ground truth regarding the metabolite levels, then the conventional basis over-estimated metabolite concentrations for the spectra obtained under the inhomogeneous B_0 field conditions: medium and poor shim groups (see Fig. 3A), whereas the water lineshape basis gave similar estimates over the linewidth range examined. LCModel considers an additional line broadening term with a Voigt lineshape, which is the product of Lorentzian and Gaussian forms, to take into account the B_0 field inhomogeneity induce broad lineshape. More importantly, LCModel finds the best compromise between the broad *in-vivo* peak and model utilizing the smoothest peak profile [13]. Even if, these additional line broadening terms are considered by default in the LCModel, the conventional approach quantified metabolite concentrations with greater variations than did the water lineshape basis set. Fig. 4A also substantiates the overestimation by the conventional approach as the corresponding concentration was significantly increased (*p-value* < 0.005) for the poor shim results.

The different degrees of freedom for spectral fitting appear to be a major reason for the difference between the two quantification approaches. As shown in Fig. 5, the result from each method showed significantly different baseline flexibilities, which should be nearly flat in the ideal situation, because LCModel quantified MM and lipid signals using additional non-parametric models. The flexibility of the baseline determines the degrees of freedom of the baseline correction [48]. LCModel adjusts the number of spline knots to change the spacing between knots that defines the level of freedom [3]. The loosely restricted baseline of the conventional approach confirms that this method has higher degree of freedom for fitting than the water lineshape fitting that showed a tightly restricted baseline. This baseline fluctuation is a typical pattern that the LCModel analysis shows for a broad linewidth [41]. A highly flexible baseline due to the decreased spacing between knots made it possible to closely approach the total *in-vivo* line. However, it also allows a relatively high degree of freedom in terms of the spectral fitting. For the closely approached fitting line to the *in-vivo* line, LCModel provides improved the goodness of fit by decreasing the uncertainty of the fitting result. However, improved precision does not necessarily mean that the metabolite was estimated correctly [41]. A fluctuating baseline may cause constrained phasing (see PCh line (blue) in Fig. 5A) and also overestimate metabolites. The water lineshape basis set showed a flatter baseline, which is characteristic of a narrow linewidth, even though the linewidth of the *in-vivo* spectrum is broad (see Fig. 5B). Even if T_2 relaxation times of the water and metabolites differ, the measured linewidths are similar for all shim conditions (see Table 1). In practice, the lineshape is dominated by T_2' at the ultrahigh field, and the T_2 contribution can be neglected. In comparison with the conventional basis set, the water lineshape basis set has a largely identical lineshape to the resultant spectra. Hence the line broadening part of the fitting algorithm will accommodate the lineshape thus limiting the degrees of freedom, and reducing the risk of over- or under-fitting.

LCModel allows the modification of the baseline flexibility via a hidden menu. In this study, we tested the effect of modifying the control parameter with regard to the baseline flexibility. When the restricted baseline estimation was used, the baseline of the conventional basis set showed similar fluctuation levels to those of the water lineshape basis set. A constrained baseline for the conventional basis set showed an improved quantification performance in terms of accuracy and stability in comparison with the conventional method (see Fig. 3). However, the improvement was inferior to that of the water lineshape method (see Fig. 4). Moreover, the arbitrarily constrained baseline failed to detect all metabolites detected by the other approaches when B_0 field was not homogeneous. We hence conclude that the water lineshape method is generally superior to the modified conventional method.

The LCModel estimates the goodness-of-fit in the output results according to the CRLB [3]. This index helps in assessing the precision of the spectral fitting method. It is widely accepted that a typical exclusion cut-off for this index is 30% [49–51]. However, recently Kreis [45] pointed out that the relative CRLB as a standard index has a limitation for use as an exclusion criterion because low concentration metabolites necessarily show high CRLB values. For this reason, we included all detected metabolites for the analyses irrespective of CRLB. A relatively broadened and flattened spectral lineshape due to poor field inhomogeneity compared to that of the good-shim spectrum has insufficient information to detect a signal with high precision, resulting in relatively larger fitting error. This explanation is commonly applied regardless of fitting methods. As shown in our results (see Fig. 4B), the mean CRLB increases as the linewidth broadens for both fitting approaches. Nevertheless, the water lineshape approach showed a higher mean of CRLB than the conventional approach. The poorer fitting quality for the water lineshape can be explained by two reasons: the water lineshape fitting shows higher CRLB for most metabolites (see Fig. 3B) regardless of the field inhomogeneity. In addition, this approach detects additional metabolites with relatively high CRLB values (above 30%) that were not detected by the conventional fitting method (see Fig. 6). Increase the CRLB value of the water lineshape method was mainly driven by these two factors.

For the range of linewidths used in this study and under the assumption that an adequate water suppression can still be achieved, this study shows that the results obtained are considerably less sensitive to the linewidth for water lineshape fitting compared to the case of the conventional spectral fitting method. The spectral quantification procedure decomposes individual metabolites from the predefined *in-vivo* signal as a post-processing step. An error in the estimate of one metabolite can affect the estimates of others. Although this water lineshape approach is less precise compared to the conventional approach, considering the fundamental objective of proton spectroscopy, the water lineshape fitting approach is superior to the conventional approach in terms of accuracy.

Our initial motivation for using the water lineshape method was to minimize differences between *in-vivo* and fitted model lineshapes so that LCModel quantification is less affected by the actual lineshape. In addition, we assumed that water lineshape is able to correct the lineshape better than mathematical algorithms since the lineshape modification by the B_0 field inhomogeneity is not specified and increasing the number of correction steps may cause over- or under-fitting. As the water lineshape method also relies on the lineshape correction algorithms that are inherent to LCModel (i.e., we did not turn off any lineshape and line broadening steps), the water lineshape method augments LCModel. The improvement in the stable metabolite concentration over the total metabolites confirms that the water lineshape approach in combination with LCModel fitting can be used for effective spectral estimation with enhanced accuracy in situations involving a wide linewidth.

Acknowledgments

This work was funded by the Helmholtz Alliance ICEMED – Imaging and Curing Environmental Metabolic Diseases, through the Initiative and Networking Fund of the Helmholtz Association.

Appendix A. Supplementary material

Supplementary data to this article can be found online at https://doi.org/10.1016/j.jmr.2019.05.002.

References

[1] D. Stefan, F. Di Cesare, A. Andrasescu, E. Popa, A. Lazariev, E. Vescovo, O. Strbak, S. Williams, Z. Starcuk, M. Cabanas, Quantitation of magnetic resonance spectroscopy signals: the jMRUI software package, Meas. Sci. Technol. 20 (2009) 104035.
[2] M. Wilson, G. Reynolds, R.A. Kauppinen, T.N. Arvanitis, A.C. Peet, A constrained least-squares approach to the automated quantitation of in vivo 1H magnetic resonance spectroscopy data, Magn. Reson. Med. 65 (2011) 1–12.
[3] S.W. Provencher, Estimation of metabolite concentrations from localized in vivo proton NMR spectra, Magn. Reson. Med. 30 (1993) 672–679.
[4] Z. Starčuk, J. Starčuková, Quantum-mechanical simulations for in vivo MR spectroscopy: principles and possibilities demonstrated with the program NMRScopeB, Anal. Biochem. (2016).
[5] K. Uğurbil, G. Adriany, P. Andersen, W. Chen, M. Garwood, R. Gruetter, P.-G. Henry, S.-G. Kim, H. Lieu, I. Tkac, Ultrahigh field magnetic resonance imaging and spectroscopy, Magn. Reson. Imag. 21 (2003) 1263–1281.
[6] P. Chang, S. Nassirpour, A. Henning, Modeling real shim fields for very high degree (and order) B0 shimming of the human brain at 9.4 T, Magn. Reson. Med. 79 (2018) 529–540.
[7] C. Lemke, A. Hess, S. Clare, V. Bachtiar, C. Stagg, P. Jezzard, U. Emir, Two-voxel spectroscopy with dynamic B0 shimming and flip angle adjustment at 7 T in the human motor cortex, NMR Biomed. 28 (2015) 852–860.
[8] A. De Graaf, J. Van Dijk, W. BoéE, QUALITY: quantification improvement by converting lineshapes to the Lorentzian type, Magn. Reson. Med. 13 (1990) 343–357.
[9] Z. Dong, Y. Zhang, F. Liu, Y. Duan, A. Kangarlu, B.S. Peterson, Improving the spectral resolution and spectral fitting of 1H MRSI data from human calf muscle by the SPREAD technique, NMR Biomed. 27 (2014) 1325–1332.
[10] Z. Dong, B.S. Peterson, Spectral resolution amelioration by deconvolution (SPREAD) in MR spectroscopic imaging, J. Magn. Reson. Imag. 29 (2009) 1395–1405.
[11] U. Klose, In vivo proton spectroscopy in presence of eddy currents, Magn. Reson. Med. 14 (1990) 26–30.
[12] R. Bartha, D. Drost, R. Menon, P. Williamson, Spectroscopic lineshape correction by QUECC: combined QUALITY deconvolution and eddy current correction, Magn. Reson. Med. 44 (2000) 641–645.
[13] I. Marshall, J. Higinbotham, S. Bruce, A. Freise, Use of voigt lineshape for quantification of in vivo1H spectra, Magn. Reson. Med. 37 (1997) 651–657.
[14] S.W. Provencher, Automatic quantitation of localized in vivo1H spectra with LCModel, NMR Biomed. 14 (2001) 260–264.
[15] J. Slotboom, C. Boesch, R. Kreis, Versatile frequency domain fitting using time domain models and prior knowledge, Magn. Reson. Med. 39 (1998) 899–911.
[16] A. Maudsley, Spectral lineshape determination by self-deconvolution, J. Magn. Reson., Ser B 106 (1995) 47–57.
[17] D. Sima, M.O. Garcia, J. Poullet, A. Suvichakorn, J.-P. Antoine, S. Van Huffel, D. Van Ormondt, Lineshape estimation for magnetic resonance spectroscopy (MRS) signals: self-deconvolution revisited, Meas. Sci. Technol. 20 (2009) 104031.
[18] Y. Zhang, S. Li, S. Marenco, J. Shen, Quantitative measurement of N-acetyl-aspartyl-glutamate at 3 T using TE-averaged PRESS spectroscopy and regularized lineshape deconvolution, Magn. Reson. Med. 66 (2011) 307–313.
[19] Y. Zhang, J. Shen, Soft constraints in nonlinear spectral fitting with regularized lineshape deconvolution, Magn. Reson. Med. 69 (2013) 912–919.
[20] D.M. Sima, S. Van Huffel, Regularized semiparametric model identification with application to nuclear magnetic resonance signal quantification with unknown macromolecular base-line, J. Roy. Stat. Soc. Ser. B (Stat. Methodol.) 68 (2006) 383–409.
[21] N. Li, L. An, J. Shen, Spectral fitting using basis set modified by measured B0 field distribution, NMR Biomed. 28 (2015) 1707–1715.
[22] V. Adalid, A. Döring, S.P. Kyathanahally, C.S. Bolliger, C. Boesch, R. Kreis, Fitting interrelated datasets: metabolite diffusion and general lineshapes, Magn. Reson. Mater. Phys., Biol. Med. 30 (2017) 429–448.
[23] A. Maudsley, A. Darkazanli, J. Alger, L. Hall, N. Schuff, C. Studholme, Y. Yu, A. Ebel, A. Frew, D. Goldgof, Comprehensive processing, display and analysis for in vivo MR spectroscopic imaging, NMR Biomed. 19 (2006) 492–503.
[24] R.F. Schulte, P. Boesiger, ProFit: two-dimensional prior-knowledge fitting of J-resolved spectra, NMR Biomed. 19 (2006) 255–263.
[25] P.A. Bottomley, J.R. Griffiths, Handbook of Magnetic Resonance Spectroscopy in vivo: MRS Theory, Practice and Applications, John Wiley & Sons, 2016.
[26] K. Levenberg, A method for the solution of certain non-linear problems in least squares, Q. Appl. Math. 2 (1944) 164–168.
[27] M. Bühl, T. van Mourik, NMR spectroscopy: quantum-chemical calculations, Wiley Interdiscip. Rev. Comput. Mol. Sci. 1 (2011) 634–647.
[28] R. Ordidge, I. Cresshull, The correction of transient B0 field shifts following the application of pulsed gradients by phase correction in the time domain, J. Magn. Reson. 69 (1986) (1969) 151–155.
[29] G.A. Morris, Compensation of instrumental imperfections by deconvolution using an internal reference signal, J. Magn. Reson. 80 (1988) (1969) 547–552.
[30] A.A. Maudsley, Evaluation of variable line-shape models and prior information in automated 1H spectroscopic imaging analysis, Magn. Reson. Med. 52 (2004) 1246–1254.
[31] B.J. Soher, K. Young, V. Govindaraju, A.A. Maudsley, Automated spectral analysis III: application to in vivo proton MR spectroscopy and spectroscopic imaging, Magn. Reson. Med. 40 (1998) 822–831.
[32] R. Kreis, J. Slotboom, L. Hofmann, C. Boesch, Integrated data acquisition and processing to determine metabolite contents, relaxation times, and macromolecule baseline in single examinations of individual subjects, Magn. Reson. Med. 54 (2005) 761–768.

[33] J.P. Mugler, J.R. Brookeman, Three-dimensional magnetization-prepared rapid gradient-echo imaging (3D MP RAGE), Magn. Reson. Med. 15 (1990) 152–157.
[34] T.W. Scheenen, D.W. Klomp, J.P. Wijnen, A. Heerschap, Short echo time 1H-MRSI of the human brain at 3T with minimal chemical shift displacement errors using adiabatic refocusing pulses, Magn. Reson. Med. 59 (2008) 1–6.
[35] T.W. Scheenen, A. Heerschap, D.W. Klomp, Towards 1H-MRSI of the human brain at 7T with slice-selective adiabatic refocusing pulses, Magn. Reson. Mater. Phys., Biol. Med. 21 (2008) 95.
[36] R. Gruetter, I. Tkáč, Field mapping without reference scan using asymmetric echo-planar techniques, Magn. Reson. Med. 43 (2000) 319–323.
[37] V. Govindaraju, K. Young, A.A. Maudsley, Proton NMR chemical shifts and coupling constants for brain metabolites, NMR Biomed. 13 (2000) 129–153.
[38] V. Govind, K. Young, A.A. Maudsley, Corrigendum: Proton NMR chemical shifts and coupling constants for brain metabolites. Govindaraju V, Young K, Maudsley AA, NMR Biomed. 2000; 13: 129–153, NMR Biomed. 28 (2015) 923–924.
[39] S. Cavassila, S. Deval, C. Huegen, D. Van Ormondt, D. Graveron-Demilly, Cramer-Rao bound expressions for parametric estimation of overlapping peaks: influence of prior knowledge, J. Magn. Reson. 143 (2000) 311–320.
[40] S. Cavassila, S. Deval, C. Huegen, D. Van Ormondt, D. Graveron-Demilly, Cramér-Rao bounds: an evaluation tool for quantitation, NMR Biomed. Int. J. Devot. Develop. Appl. Magn. Reson. In Vivo 14 (2001) 278–283.
[41] Y. Zhang, J. Shen, Smoothness of in vivo spectral baseline determined by mean-square error, Magn. Reson. Med. 72 (2014) 913–922.
[42] M.A. Brown, Time-domain combination of MR spectroscopy data acquired using phased-array coils, Magn. Reson. Med. 52 (2004) 1207–1213.
[43] S.W. Provencher, LCModel & LCMgui user's manual, LCModel Version, 2016, pp. 6.3-1L.
[44] B. Bank, U. Emir, V. Boer, J. Asten, M. Maas, J. Wijnen, H. Kan, G. Oz, D. Klomp, T. Scheenen, Multi-center reproducibility of neurochemical profiles in the human brain at 7 T, NMR Biomed. 28 (2015) 306–316.
[45] R. Kreis, The trouble with quality filtering based on relative Cramér-Rao lower bounds, Magn. Reson. Med. 75 (2016) 15–18.
[46] M.G. Soeiro-de-Souza, B.F. Pastorello, C.d.C. Leite, A. Henning, R.A. Moreno, M. C. Garcia Otaduy, Dorsal anterior cingulate lactate and glutathione levels in euthymic bipolar I disorder: 1H-MRS study, Int. J. Neuropsychopharmacol. 19 (2016).
[47] D. Belkic, K. Belkic, Signal Processing in Magnetic Resonance Spectroscopy with Biomedical Applications, CRC Press, 2010.
[48] S. Pradhan, B.J. Soher, P.B. Barker, Quantifying Spectra in the Frequency Domain, eMagRes (2016).
[49] B.R. Godlewska, A. Pike, A.L. Sharpley, A. Ayton, R.J. Park, P.J. Cowen, U.E. Emir, Brain glutamate in anorexia nervosa: a magnetic resonance spectroscopy case control study at 7 Tesla, Psychopharmacology (Berlin) 234 (2017) 421–426.
[50] M. Považan, B. Strasser, G. Hangel, E. Heckova, S. Gruber, S. Trattnig, W. Bogner, Simultaneous mapping of metabolites and individual macromolecular components via ultra-short acquisition delay 1H MRSI in the brain at 7T, Magn. Reson. Med. 79 (2018) 1231–1240.
[51] K. Dyke, S.E. Pépés, C. Chen, S. Kim, H.P. Sigurdsson, A. Draper, M. Husain, P. Nachev, P.A. Gowland, P.G. Morris, Comparing GABA-dependent physiological measures of inhibition with proton magnetic resonance spectroscopy measurement of GABA using ultra-high-field MRI, Neuroimage 152 (2017) 360–370.